THE JOURNAL OF PHYSICAL CHEMISTRY Letters

Letter

pubs.acs.org/JPCL

Compressed Sensing for Multidimensional Spectroscopy Experiments

Jacob N. Sanders,[†] Semion K. Saikin,[†] Sarah Mostame,[†] Xavier Andrade,[†] Julia R. Widom,[‡] Andrew H. Marcus,[‡] and Alán Aspuru-Guzik*,[†]

[†]Department of Chemistry and Chemical Biology, Harvard University, Cambridge, Massachusetts 02138, United States

[‡]Department of Chemistry, Oregon Center for Optics, Institute of Molecular Biology, University of Oregon, Eugene, Oregon 97403, United States

ABSTRACT: Compressed sensing is a processing method that significantly reduces the number of measurements needed to accurately resolve signals in many fields of science and engineering. We develop a two-dimensional variant of compressed sensing for multidimensional spectroscopy and apply it to experimental data. For the model system of atomic rubidium vapor, we find that compressed sensing provides an order-of-magnitude (about 10-fold) improvement in spectral resolution along each dimension, as compared to a conventional discrete Fourier transform, using the same data set. More attractive is that compressed sensing allows for random undersampling of the experimental data, down to less than 5% of the experimental data set, with essentially no loss in spectral resolution. We believe that by combining powerful resolution with ease of use, compressed sensing can be a powerful tool for the analysis and interpretation of ultrafast spectroscopy data.

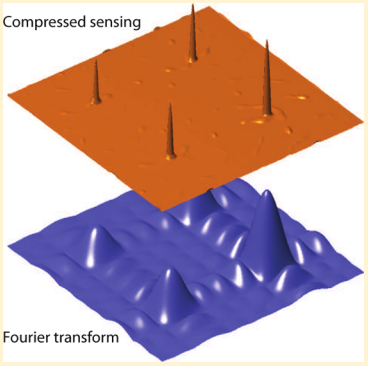

SECTION: Spectroscopy, Photochemistry, and Excited States

Compressed sensing (CS) is a state-of-the-art signal processing method that has recently become popular throughout the physical and biological sciences. The method is founded on the concept of *sparsity*. When a signal is known to be sparse in a certain basis (i.e., most of the coefficients are negligibly small), this knowledge can be used to dramatically reduce the number of measurements required to reconstruct the signal.[1,2] This method has been applied to many areas of research, ranging from magnetic resonance imaging[3] to superresolved imaging of single molecules[4] and quantum process tomography.[5]

In this Letter, we present the application of CS to experimental ultrafast two-dimensional (2D) optical spectroscopy. Multidimensional spectroscopy[6−9] is an important tool for studying ultrafast dynamical processes in complex molecular systems. For instance, it can be used to analyze vibrational energy transfer at liquid/air interfaces on picosecond time scales[10] or exciton dynamics in natural light harvesting systems at hundreds of femtoseconds.[11−13] It can also be applied to the efficient detection and identification of molecules, which is one of the crucial challenges in chemistry, biology, and medicine with important applications to molecular sensing, chemical separation, and DNA analysis.[14,15] Frequently, in these nonlinear optical techniques, the data is collected in the time domain, and then Fourier transformed to the frequency domain.

While the Fourier transform (FT) is a standard technique in optical spectroscopy, different data processing methods have been applied previously mainly in nuclear magnetic resonance (NMR) spectral analysis.[16,17] All these techniques can be classified into two main groups: (a) methods requiring periodic sampling, such as the discrete FT[18,19] and linear prediction (LP)[16,20] including its variations;[21] and (b) methods that use nonuniform sampling strategies, for instance maximum entropy methods (see references in ref 17). Formally, the CS method belongs to the latter group, where either random or periodic sampling is applied with no preassumptions about the shape of the signal besides its sparsity. The main drawback of periodic sampling methods is the dual constraint on data collection: long time data collection is required to obtain good spectral resolution, while closely spaced sample points are needed to avoid aliasing. Nonuniform sampling methods can alleviate these issues, but sometimes introduce sampling artifacts.[17]

Earlier, some of us showed that CS can also be used to significantly reduce the computational cost of atomistic simulations.[22] In that work, the application of CS was particularized for molecular dynamics and real-time time-dependent density functional theory simulations for obtaining linear spectra (vibrational, optical absorption, and circular dichroism).[23] However, CS can be applied to other types of simulations and experimental techniques. Multidimensional nonlinear spectroscopy is an interesting and relevant candidate to explore the possibilities of CS. Recently, CS has been pursued for the reconstruction of one of the dimensions in 2D NMR data[24] and for the theoretical simulation of 2D spectra.[25]

Received: July 19, 2012
Accepted: September 4, 2012
Published: September 4, 2012

   dx.doi.org/10.1021/jz300988p | *J. Phys. Chem. Lett.* 2012, 3, 2697−2702

As an illustration we apply the method to an experimental system, atomic Rubidium vapor, which is frequently used as a test model for multidimensional spectroscopy techniques.[26−28] Many multidimensional experiments are inherently limited in the amount of time-domain data that may be collected, either due to measurement constraints or to more fundamental limitations such as the time scale of the dynamics one wishes to explore (which may be very short due to decoherence and other processes). We believe CS can extend the range of spectroscopically observable dynamics from limited time domain data. Here, we show that CS resolves spectral lines about an order-of-magnitude better as compared to a discrete FT using the same data set. While CS can be applied with a uniform sampling strategy, the full potential of the method is realized when a nonuniform random sampling is adopted.[2] In particular, we find that CS with random undersampling down to only 5% of the data yields spectra that are comparable in resolution to those obtained using all of the experimental data.

Another benefit of CS is that it is quite easy for experimentalists to integrate into existing schemes. As discussed below, our basic approach simply replaces the 2D discrete FT by a new 2D CS scheme. It is our hope that CS's easy portability will help it become a common method among experimental spectroscopists.

The rest of this Letter is structured as follows: We first present the CS method and outline its application to the resolution of 2D ultrafast optical spectra. Next, we apply the method to a model experimental system, namely, gas-phase Rubidium atoms, and show how CS can be used to obtain a 10-fold improvement in spectral resolution as compared to FT. We then turn to the effects of different sampling patterns on signal reconstruction, focusing on how random undersampling can be used without sacrificing spectral resolution. Finally, we offer conclusions and a future outlook.

We begin by describing how the CS method can be applied to 2D ultrafast optical spectroscopy (see refs 29−31 for more detailed information about CS). As an illustration, we focus on four-wave mixing experiments, similar to those used to study coherent energy transfer in light-harvesting complexes, quantum dots, and other systems of physical and biological interest. Our experimental setup involves irradiating a sample with four optical pulses and varying the time gaps between the pulses (Figure 1). Defining the time gaps as τ (the coherence time between pulses 1 and 2), T (the population time between pulses 2 and 3), and t (the detection time between pulses 3 and 4), the signal measured in the time domain is a function $h(\tau, T, t)$. The standard approach is to perform a 2D discrete FT in τ and t to obtain the frequency spectrum $g(\omega, T, w)$

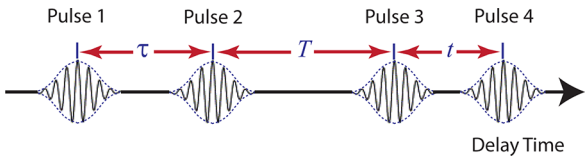

Figure 1. Schematic illustration of the sequence of four pulses used in 2D optical spectroscopy.

$$g(\omega, T, w) = \int \mathrm{d}\tau\ \mathrm{d}t e^{i\omega\tau} e^{iwt} h(\tau, T, t) \tag{1}$$

This frequency spectrum is typically plotted in $\omega-w$ space for different values of T, and the dynamics of the peaks then give information about the dynamics of the underlying system.

It has been shown previously how the CS method can be used to replace a *one*-dimensional discrete FT in converting time-resolved data into the frequency domain,[1,22] obtaining a significantly better frequency resolution. Our basic approach here is to generalize the method to the 2D case. A higher multidimensional CS scheme can also be obtained as a straightforward generalization.

For 2D spectroscopy the measurement is usually done for a finite set of points $\{(\tau_j, t_k)\}$ arranged on a $N_\tau \times N_t$ grid. We call the set of measured time-resolved values $\boldsymbol{h} = \{h_{[jk]}\}$. To obtain the 2D spectra we need to calculate the associated set of Fourier coefficients $\boldsymbol{g} = \{g_{[lm]}\}$ defined on a grid of $N_\omega \times N_w$ points $\{(\omega_l, w_m)\}$ in frequency space. This can be done by using a discrete FT

$$g_{[lm]} = \sum_{j=1}^{N_\tau} \sum_{k=1}^{N_t} \Delta\tau \Delta t e^{i\omega_l \tau_j} e^{iw_m t_k} h_{[jk]} \tag{2}$$

where $\Delta\tau$ and Δt are the values of the spacing of the 2D time grid.

However, if many of the frequency components are zero, then we only need a number of samples proportional to the number of nonzero coefficients in the spectrum;[2] this is the fundamental principle behind CS. The CS approach imposes sparsity as an additional requirement to the determination of the Fourier coefficients, thereby significantly reducing the number of samples required for a well-resolved spectrum. We start by reformulating the 2D discrete FT in eq 2 as a linear problem. From this perspective, we are solving the linear equation for $\mathbf{g}$,

$$F\mathbf{g} = \mathbf{h} \tag{3}$$

where F is the $(N_\omega N_w) \times (N_\tau N_t)$ inverse Fourier matrix with entries

$$F_{[jk][lm]} = \frac{4}{\pi^2} \Delta\omega \Delta w e^{-i\omega_l \tau_j} e^{-iw_m t_k} \tag{4}$$

Our objective is to obtain sensible results with N_τ and N_t as small as possible, so the linear problem is underdetermined $(N_\omega N_w > N_\tau N_t)$ and as such it has many solutions. From all of them we select the sparsest one: the solution with the largest number of zero coefficients. In practice, this solution can be obtained by solving the basis-pursuit denoising (BPDN) problem[1]

$$\min_{\mathbf{g}} |\mathbf{g}|_1 \quad \text{subject to} \quad |F\mathbf{g} - \mathbf{h}|_2 < \eta \tag{5}$$

where the 1-norm $|\mathbf{g}|_1 = \sum_{[jk]} |g_{[jk]}|$ is used. The η value accounts for a certain level of noise that can be present in the experimental data. In all calculations that follow, we set $\eta < 10^{-4}$.

As an example, we consider phase-modulation 2D fluorescence spectroscopy (PM-2DFS) data collected from atomic ^{87}Rb vapor.[28] The lowest electronic transitions in ^{87}Rb gas may be considered as a quantum three-level system with ground state $5\ ^2S_{1/2}$, first excited state $5\ ^2P_{1/2}$, and second excited state $5\ ^2P_{3/2}$, as illustrated in Figure 2. The four light pulses are produced by a titanium saphire laser [with full width at half-maximum (fwhm) ∼ 42 fs] that is resonant with electronic transitions of ^{87}Rb: $5\ ^2S_{1/2} \rightarrow 5\ ^2P_{1/2}$ (with transition

dx.doi.org/10.1021/jz300988p | J. Phys. Chem. Lett. 2012, 3, 2697−2702

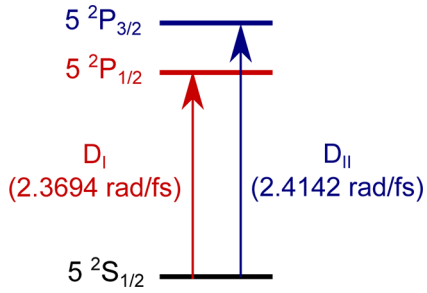

Figure 2. Energy level diagram for atomic ^{87}Rb vapor. The transition frequencies are obtained from ref 34.

frequency 2.3694 rad/fs) and 5 $^2S_{1/2} \rightarrow 5\ ^2P_{3/2}$ (with transition frequency 2.4142 rad/fs). We considered ^{87}Rb vapor to be an ideal candidate for our 2D CS method, as its 2D electronic spectrum is expected to be sparse in frequency space, with diagonal and cross peaks corresponding to the transitions just mentioned. The natural lifetime of electronic excitations in ^{87}Rb is about 25 ns, which corresponds to very narrow natural linewidths (D_I = 36.1 and D_{II} = 38.1 rad/ms). Full and extensive details of the PM-2DFS experimental method used to collect the data are given in refs 28, 32, and 33. The experiments yield time-resolved fluorescence-detected "sum" and "difference" signals [$h_{sum}(\tau, T, t)$ and $h_{diff}(\tau, T, t)$] that are analogous, respectively, to the nonrephasing and rephasing third-order polarizations collected in more traditional four-wave mixing experiments. In the rest of this paper, we focus on the "difference" (rephasing) signal obtained for population time T = 140 fs. We have observed exactly the same improvements upon applying our 2D CS method to other population times and to "sum" (nonrephasing) signals.

The main results of this letter are summarized in Figures 3−5, which compare the performance of the 2D discrete FT and our 2D CS method, with both uniform and random sampling, in resolving the spectral peaks corresponding to transitions in the atomic ^{87}Rb vapor. Several conclusions about 2D CS may be drawn by systematically comparing different parts of the figures.

The first important comparison is between panels a and b of Figure 3. These two panels present the results of applying the 2D FT and 2D CS methods to exactly the same set of time-domain experimental data (a grid of 25 evenly spaced points in τ and 25 evenly spaced points in t with $\Delta\tau = \Delta t$ = 26.7 fs, for a total sampling time of 667 fs in each time dimension). We see that CS produces peaks that are better resolved in frequency space than those obtained by the discrete FT from exactly the same data. In fact, the CS peaks are better resolved by an order of magnitude (about 10 times) along each dimension, consistent with the results we previously obtained for one-dimensional spectra.[22] In Figure 3c, we compute the 2D spectrum using a randomly selected subset of 25^2 data points from the entire 45 × 45 grid of available time-domain data. While this is not a full random sampling on the continuous space, it allows us to use the same data to investigate the effects of random sampling in CS.

The advantage of 2D CS over 2D FT is quantified in Figure 4. This graph compares the line width of the upper-right peak obtained by FT (black) and CS (red) while varying the number of time points sampled in each dimension. Since the density of time points is held constant, this corresponds to varying the total experimental sampling time along the τ and t dimensions.

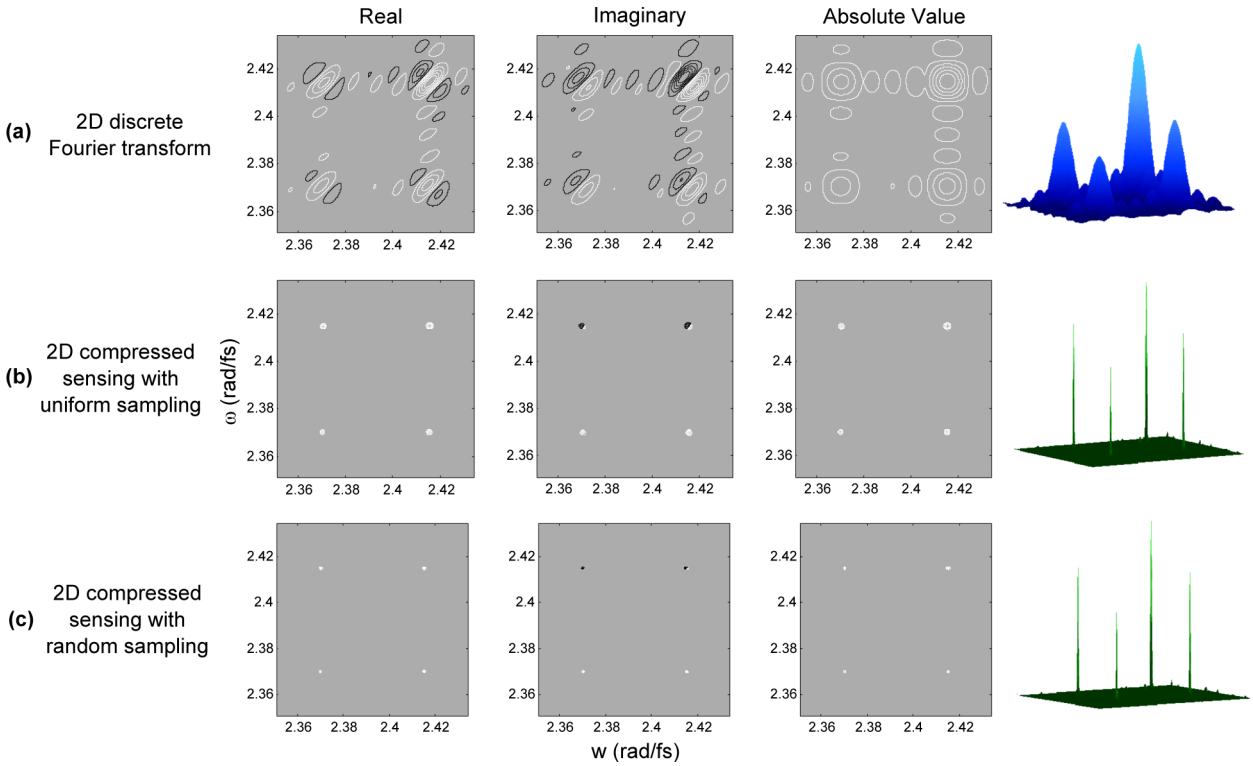

Figure 3. Comparison between FT and CS, with both uniform and random sampling, in resolving the 2D optical spectrum of gas-phase atomic Rb at a population time of T = 140 fs. (a) FT using a uniform time grid of 25 × 25 evenly spaced points with $\Delta\tau = \Delta t$ = 26.7 fs. (b) CS using exactly the same time-domain data as panel a. (c) CS using random sampling of 25^2 time points drawn from full grid of 45 × 45 time points.

dx.doi.org/10.1021/jz300988p | J. Phys. Chem. Lett. 2012, 3, 2697−2702

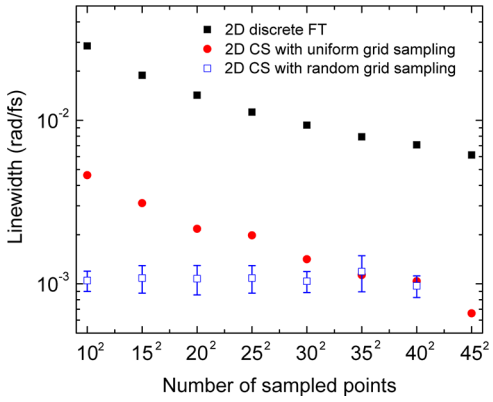

Figure 4. Comparison of linewidths obtained using FT and CS, with both uniform and random sampling, as the number of time-domain measurements is varied. The discrete FT (black) and the CS with uniform grid sampling (red) are done using the first N^2 evenly spaced points on a 2D time grid with $\Delta\tau = \Delta t = 26.7$ fs. The CS with random grid sampling (blue) is done using N^2 points drawn randomly from the entire 45 × 45 time grid. Linewidths are reported as the mean of the widths along the ω and w axes. For each random sampling data point, linewidths are averaged over 10 different random samplings; error bars denote the standard deviation.

As expected, for longer sampling times, the peaks become narrower and better resolved with both FT and CS methods. However, CS consistently provides an order of magnitude improvement over the discrete FT for a given sampling time. In fact, applying CS to the first 10 time points along each dimension (total sampling time 267 fs) yields higher spectral resolution than applying the discrete FT to 45 time points along each dimension (total sampling time 1201 fs).

In Figure 4 we also compare the linewidths generated by the random-sampling CS approach (blue dots). For each point we average over 10 different sets of random samples. As shown in the figure, random sampling drastically reduces the number of time-domain measurements needed to obtain well-resolved spectra, even beyond what can be achieved by using CS with uniform sampling. Even randomly sampling only 10^2 points (about 5% of the total number of points) in the time-domain (the far-left blue point), we obtain linewidths that are not much larger than sampling the entire data set of 45^2 points (the far-right red point). In other words, randomly undersampling from the time-domain grid provides nearly the same spectral resolution as if the entire grid was sampled and the spectral resolution does not change much as the extent of random undersampling increases. Note, however, that attempting to sample 5^2 points resulted in failed spectral reconstruction; the extent of undersampling that is permissible is known to scale with the sparsity of the signal to be reconstructed.[2] It is reasonable to expect that a fully random CS approach would provide even better resolution in comparison with selecting random points from a grid as done in these calculations.

Finally, to confirm the accuracy of FT and CS, with both uniform and random sampling, we computed the error in the frequency difference between the two optical transitions (Figure 5a) and the error in the average frequency of these transitions (Figure 5b) for all three methods. In all cases, both the average and the difference of the frequencies fall within a few frequency grid points of the true values (the true values are 0.0448 rad/fs for the frequency difference and 2.3918 rad/fs for the frequency average[34]). Moreover, while the uniform CS sampling gives a small improvement over the discrete FT, the random CS sampling provides more accurate frequency differences and average frequencies even using a minimal number of time-domain measurements.

Uniform CS sampling with reduced density of the grid points, for example, by sampling every Nth time point, results in aliasing once the frequency bandwidth is smaller than the energy difference between the highest-energy and lowest-energy peaks (similar to discrete FT). Random CS sampling, by contrast, provides the best of both worlds: a way to decrease the average sampling density without sacrificing either frequency resolution or frequency bandwidth.

Taken together, our results give a prescription for how to obtain the highest possible spectral resolution using CS. Even with our 2D CS method, the spectral resolution is still limited by the total sampling time. Though CS provides an order of magnitude improvement compared to the discrete FT, measurements collected at large τ and t will still be required

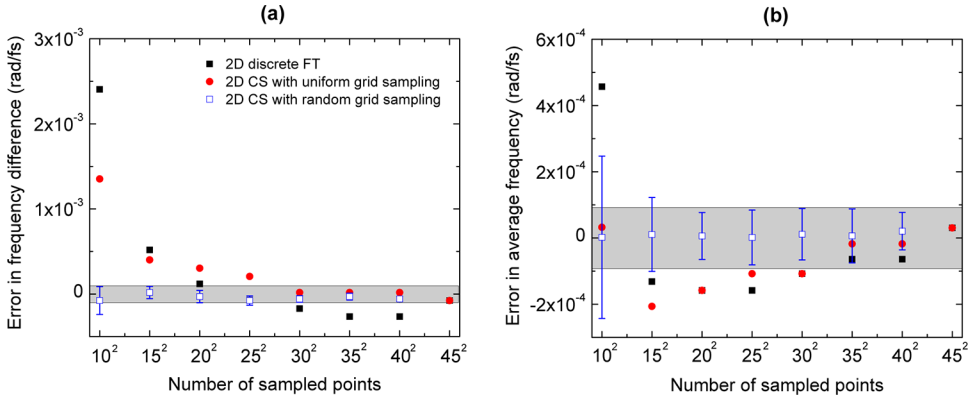

Figure 5. Comparison of (a) the error in the frequency difference between two optical transitions and (b) the error in the average frequency of these transitions obtained using FT and CS, with both uniform and random sampling, as the number of time-domain measurements is varied. The true values are 0.0448 rad/fs for the frequency difference and 2.3918 rad/fs for the frequency average. The discrete FT (black) and the CS with uniform grid sampling (red) are done using the first N^2 evenly spaced points on a 2D time grid with $\Delta\tau = \Delta t = 26.7$ fs. The CS with random grid sampling (blue) is done using N^2 points drawn randomly from the entire 45 × 45 time grid. For each random sampling data point, the frequency difference and the average frequency error are averaged over 10 different random samplings; error bars denote the standard deviation. The gray area shows "exact" positions to within the precision of our frequency grid (which has spacing 0.000189 rad/fs).

dx.doi.org/10.1021/jz300988p | J. Phys. Chem. Lett. 2012, 3, 2697−2702

to achieve high resolution. However, a major advantage of CS is that random sampling can be used to drastically cut down on the *number* of measurements needed to achieve this high resolution.

Despite the improved resolution, CS still does not resolve the natural line width of the peaks, which are very narrow. The issue of peak shape certainly deserves a more extensive investigation in the future, most likely by applying our 2D CS method to more complex experimental systems with intricate features that are broadened by internal structure or an environment. Another interesting continuation of our work would be to compare the CS with other techniques for resolving spectral lines, including LP[16,20,21] and maximum entropy methods.[35,36] Comparison to other sampling methods will require the use of many experimental signals and the development of performance metrics. This is an open research direction.

In conclusion, we have demonstrated the first application of CS to 2D optical spectroscopy experiments. Focusing on electronic transitions in an atomic ^{87}Rb vapor model system, we have shown that the 2D CS method that we have developed provides much finer resolution of the peaks in a 2D spectrum as compared to the standard discrete FT. In particular, experimentalists can apply 2D CS as a simple "drop-in" replacement for a discrete FT to obtain an order of magnitude improvement in spectral resolution from the same samples. Moreover, CS theory and our results with quasi-random sets suggest that, in order to increase even further the amount of useful information obtained per sample, a fully random sampling strategy should be adopted for experimental measurements. We expect that 2D CS will substantially reduce the experimental effort needed to obtain well-resolved spectra, increasing the range of spectral features resolvable in ultrafast experiments, particularly closely spaced peaks. We are confident that CS will become more widely investigated and employed in the 2D experimental ultrafast community once its easy portability and strong resolving power become more widely known.

METHODS

The PM-2D FS method is described in detail in ref 28. A Rb vapor cell was excited by a sequence of four collinear optical pulses with adjustable interpulse delays (see Figure 1). The transmitted beam intensity was used to determine the stage positions corresponding to $\tau = t = 0$. The fluorescence emitted from the sample was detected using an avalanche photodiode. The phases of the pulse electric fields were continuously swept at distinct frequencies using acousto-optic Bragg cells, and separate reference waveforms were constructed from the resultant intensities of pulses 1 and 2, and of pulses 3 and 4, which were set to 5 kHz and 8 kHz, respectively. The reference signals were sent to a waveform mixer to construct "sum" and "difference" sideband references (13 and 3 kHz, respectively). These sideband references were used to phase-synchronously detect the fluorescence. All measurements were carried out at room temperature.

Time-resolved "sum" and "difference" signals were collected at all points on a 2D grid consisting of 45 equally spaced coherence times τ and 45 equally spaced detection times t (with $\Delta\tau = \Delta t = 26.7$ fs) for a series of 5 population times T = 140, 175, 210, 245, and 280 fs. In this paper, we analyzed the "difference" signal obtained at T = 140 fs, although similar results were obtained for different population times as well as for "sum" signals.

For both the FT and CS calculations, we use a 2D frequency grid consisting of 500 evenly spaced points between $-2\pi/(5\Delta\tau)$ and $2\pi/(5\Delta\tau)$ for ω and 500 evenly spaced points between $-2\pi/(5\Delta t)$ and $2\pi/(5\Delta t)$ for w. This corresponds to a frequency spacing of $\Delta\omega = \Delta w = 0.000189$ rad/fs. This frequency grid is wide enough to contain all of the peaks present in the spectrum. (For more robust numerical stability, in all CS calculations, we surrounded this grid by a coarser grid with 100 evenly spaced points in each dimension covering the entire frequency range $[-\pi/\Delta\tau, \pi/\Delta\tau] \times [-\pi/\Delta t, \pi/\Delta t]$, excluding the part already covered by the finer grid.)

Performing the 2D CS calculations involves solving the optimization problem in eq 5 for different amounts of uniformly sampled and randomly sampled time-domain data as described in the text. Solving this optimization problem is not trivial, so we rely on the spectral projected gradient for 1-norm minimization (SPGL1) algorithm developed by van den Berg and Friedlander, which is available as free and open-source MatLab code.[37] To avoid numerical stability issues, we work with a normalized BPDN problem, where the prefactor $(4\Delta\omega\Delta w/\pi^2)$ of the F matrix, eq 4, is left out and $\mathbf{h}$ is normalized. The missing factors are included in $\mathbf{g}$ after the solution is found.

AUTHOR INFORMATION

Corresponding Author

*E-mail: aspuru@chemistry.harvard.edu.

Notes

The authors declare no competing financial interest.

ACKNOWLEDGMENTS

We acknowledge J. Yuen-Zhou and J. Goodknight for useful discussions. The computations in this paper were run on the Odyssey cluster supported by the FAS Science Division Research Computing Group at Harvard University. J.N.S. acknowledges support from the Department of Defense (DoD) through the National Defense Science & Engineering Graduate Fellowship (NDSEG) Program. A.H.M. acknowledges grants from the Office of Naval Research (N00014-11-1-0193) and from the National Science Foundation, Chemistry of Life Processes Program (CHE-1105272). A.A.-G. acknowledges the support of the Defense Threat Reduction Agency under Contract No HDTRA1-10-1-0046 and the Defense Advanced Research Projects Agency under award number N66001-10-1-4060. Further, A.A.-G. is grateful for the support of the Harvard Quantum Optics Center, the Camille and Henry Dreyfus Foundation, and the Alfred P. Sloan Foundation.

REFERENCES

(1) Candes, E.; Romberg, J.; Tao, T. Robust Uncertainty Principles: Exact Signal Reconstruction from Highly Incomplete Frequency Information. *IEEE Trans. Inf. Theory* **2006**, *52*, 489−509.

(2) Donoho, D. Compressed Sensing. *IEEE Trans. Inf. Theory* **2006**, *52*, 1289−1306.

(3) Lustig, M.; Donoho, D.; Pauly, J. M. Sparse MRI: The Application of Compressed Sensing for Rapid MRI Imaging. *Magnet. Reson. Med.* **2007**, *58*, 1182−1195.

(4) Zhu, L.; Zhang, W.; Elnatan, D.; Huang, B. Faster STORM Using Compressed Sensing. *Nat. Methods* **2012**, *9*, 721−723.

(5) Shabani, A.; Kosut, R. L.; Mohseni, M.; Rabitz, H.; Broome, M. A.; Almeida, M. P.; Fedrizzi, A.; White, A. G. Efficient Measurement of

Quantum Dynamics via Compressive Sensing. *Phys. Rev. Lett.* **2011**, *106*, 100401.
(6) Hochstrasser, R. M. Multidimensional Ultrafast Spectroscopy Special Feature: Multidimensional Ultrafast Spectroscopy. *Proc. Natl. Acad. Sci. U.S.A.* **2007**, *104*, 14189.
(7) Hamm, P.; Hochstrasser, R. M. In *Ultrafast Infrared and Raman Spectroscopy*; Fayer, M. D., Ed.; Marcel Dekker, 2001; pp 273−347.
(8) Khalil, M.; Demirdöven, N.; Tokmakoff, A. Coherent 2D IR Spectroscopy: Molecular Structure and Dynamics in Solution. *J. Phys. Chem. A* **2003**, *107*, 5258−5279.
(9) Jonas, D. M. Two-Dimensional Femtosecond Spectroscopy. *Annu. Rev. Phys. Chem.* **2003**, *54*, 425−463.
(10) Zhang, Z.; Piatkowski, L.; Bakker, H. J.; Bonn, M. Ultrafast Vibrational Energy Transfer at the Water/Air Interface Revealed by Two-Dimensional Surface Vibrational Spectroscopy. *Nat. Chem.* **2011**, *3*, 888−893.
(11) Brixner, T.; Stenger, J.; Vaswani, H. M.; Cho, M.; Blankenship, R. E.; Fleming, G. R. Two-Dimensional Spectroscopy of Electronic Couplings in Photosynthesis. *Nature* **2005**, *434*, 625−628.
(12) Yuen-Zhou, J.; Aspuru-Guzik, A. Quantum Process Tomography of Excitonic Dimers from Two-Dimensional Electronic Spectroscopy. I. General Theory and Application to Homodimers. *J. Chem. Phys.* **2011**, *134*, 134505.
(13) Yuen-Zhou, J.; Krich, J. J.; Mohseni, M.; Aspuru-Guzik, A. Quantum State and Process Tomography of Energy Transfer Systems via Ultrafast Spectroscopy. *Proc. Natl. Acad. Sci. U.S.A.* **2011**, *108*, 17615.
(14) Mukherjee, P.; Kass, I.; Arkin, I. T.; Zanni, M. T. Picosecond Dynamics of a Membrane Protein Revealed by 2D IR. *Proc. Natl. Acad. Sci. U.S.A.* **2006**, *103*, 3528−3533.
(15) Ghosh, A.; Qiu, J.; DeGrado, W. F.; Hochstrasser, R. M. Tidal Surge in the M2 Proton Channel, Sensed by 2D IR Spectroscopy. *Proc. Natl. Acad. Sci. U.S.A.* **2011**, *108*, 6115−6120.
(16) Koehl, P. Linear Prediction Spectral Analysis of NMR Data. *Prog. Nucl. Magn. Reson. Spectrosc.* **1999**, *34*, 257−299.
(17) Mobli, M.; Maciejewski, M.; Schuyler, A.; Stern, A.; Hoch, J. Sparse Sampling Methods in Multidimensional NMR. *Phys. Chem. Chem. Phys.* **2012**, *14*, 10835−10843.
(18) Ernst, R. R.; Anderson, W. A. Application of Fourier Transform Spectroscopy to Magnetic Resonance. *Rev. Sci. Instrum.* **1966**, *37*, 93−102.
(19) Brixner, T.; Mancal, T.; Stiopkin, I.; Fleming, G. Phase-Stabilized Two-Dimensional Electronic Spectroscopy. *J. Chem. Phys.* **2004**, *121*, 4221−4236.
(20) Led, J.; Gesmar, H. Application of the Linear Prediction Method to NMR Spectroscopy. *Chem. Rev.* **1991**, *91*, 1413−1426.
(21) Tang, J.; Norris, J. LPZ Spectral Analysis Using Linear Prediction and the Z-Transform. *J. Chem. Phys.* **1986**, *84*, 5210−5211.
(22) Andrade, X.; Sanders, J. N.; Aspuru-Guzik, A. Application of Compressed Sensing to the Simulation of Atomic Systems. *Proc. Natl. Acad. Sci. U.S.A.* **2012**, *109*, 13928−13933.
(23) Andrade, X.; Alberdi-Rodriguez, J.; Strubbe, D. A.; Oliveira, M. J.; Nogueira, F.; Castro, A.; Muguerza, J.; Arruabarrena, A.; Louie, S. G.; Aspuru-Guzik, A.; Rubio, A.; Marques, M. A. L. Time-Dependent Density-Functional Theory in Massively Parallel Computer Architectures: The Octopus Project. *J. Phys.: Condens. Matter* **2012**, *24*, 233202.
(24) Shrot, Y.; Frydman, L. Compressed Sensing and the Reconstruction of Ultrafast 2D NMR Data: Principles and Biomolecular Applications. *J. Magn. Reson.* **2011**, *209*, 352−358.
(25) Almeida, J.; Prior, J.; Plenio, M. B. Computation of 2D Spectra Assisted by Compressed Sampling. *J. Phys. Chem. Lett.* **2012**, *3*, 2692−2696.
(26) Tian, P.; Keusters, D.; Suzaki, Y.; Warren, W. S. Femtosecond Phase-Coherent Two-Dimensional Spectroscopy. *Science* **2003**, *300*, 1553−1555.
(27) Vaughan, J. C.; Hornung, T.; Stone, K. W.; Nelson, K. A. Coherently Controlled Ultrafast Four-Wave Mixing Spectroscopy. *J. Phys. Chem. A* **2007**, *111*, 4873−4883.
(28) Tekavec, P. F.; Lott, G. A.; Marcus, A. H. Fluorescence-Detected Two-Dimensional Electronic Coherence Spectroscopy by Acousto-Optic Phase Modulation. *J. Chem. Phys.* **2007**, *127*, 214307.
(29) Baraniuk, R. Compressive Sensing. *IEEE Signal Process. Mag.* **2007**, *24*, 118−121.
(30) Candes, E.; Wakin, M. An Introduction To Compressive Sampling. *IEEE Signal Process. Mag.* **2008**, *25*, 21−30.
(31) Chartrand, R.; Baraniuk, R. G.; Eldar, Y. C.; Figueiredo, M. A. T.; Tanner, J. Introduction to the Issue on Compressive Sensing. *IEEE J. Sel. Top. Signal Process.* **2010**, *4*, 241−243.
(32) Lott, G. A.; Perdomo-Ortiz, A.; Utterback, J. K.; Widom, J. R.; Aspuru-Guzik, A.; Marcus, A. H. Conformation of Self-Assembled Porphyrin Dimers in Liposome Vesicles by Phase-Modulation 2D Fluorescence Spectroscopy. *Proc. Natl. Acad. Sci. U.S.A.* **2011**, *108*, 16521.
(33) Perdomo-Ortiz, A.; Widom, J.; Lott, G.; Aspuru-Guzik, A.; Marcus, A. Conformation and Electronic Population Transfer in Membrane Supported Self-Assembled Porphyrin Dimers by 2D Fluorescence Spectroscopy. *J. Phys. Chem. B* **2012**, *116*, 10757−10770.
(34) Steck, D. *Rubidium 87 D Line Data*; Theoretical Division (T-8), MS B285 Los Alamos National Laboratory: Los Alamos, NM, 2001; Available online at http://steck.us/alkalidata.
(35) Gull, S.; Daniell, G. Image Reconstruction from Incomplete and Noisy Data. *Nature* **1978**, *272*, 686−690.
(36) Stern, A. S.; Donoho, D. L.; Hoch, J. C. NMR Data Processing Using Iterative Thresholding and Minimum l(1)-Norm Reconstruction. *J. Magn. Reson.* **2007**, *188*, 295−300.
(37) van den Berg, E.; Friedlander, M. P. Probing the Pareto Frontier for Basis Pursuit Solutions. *SIAM J. Sci. Comput.* **2009**, *31*, 890−912.